ELSEVIER

Tectonophysics 271 (1997) 217–229

TECTONOPHYSICS

Diapir-driven crustal convection: decompression melting, renewal of the magma source and the origin of nested plutons

Roberto F. Weinberg [1]

Research School of Earth Sciences, Australian National University, Canberra, ACT 0200, Australia

Received 22 February 1996; accepted 30 October 1996

Abstract

This paper studies numerically the rise of diapirs and the consequences of diapir-driven crustal flow. The ascent of diapirs imposes a convective flow pattern concentrated mostly in the low-viscosity lower crust in which the rocks immediately surrounding the diapir are dragged upwards and rocks a few radii to the sides of the diapir are pushed downwards to fill the gap left by the rising mass. There are two main consequences of this flow. One, warm and water undersaturated rocks may undergo decompression melting when dragged upwards. This is shown to enhance the ability of a diapir to intrude the crust, because the partially molten wall rocks gain buoyancy and add to the total buoyancy of the diapir, which regains part of the energy it spent on heating and dragging the surroundings. Two, the downward flow of rocks renews the magma source with potentially fertile rocks, which may undergo melting and give rise to a new diapir which will follow the same path as the first one and repeat the process, giving rise to a sequence of diapirs. Whereas source renewal is a direct result of diapirism, magma transport through dykes leads to the accumulation of refractory restite in the source which will eventually prevent further melting. Diapirism and decompression melting may lead to strong recycling of the lower crust and give rise to large volumes of melt. Sequential diapirism may explain nested plutons and multipulse mid- to upper-crustal batholiths.

Keywords: diapirs; decompression; melting; convection

1. Introduction

The mechanisms of magma ascent and emplacement in the crust have been widely debated in the literature (e.g., Clemens and Mawer, 1992; Paterson and Fowler, 1993; Brown, 1994; Weinberg, 1994; Weinberg and Podladchikov, 1994). Debate concentrates on whether felsic plutons are a result of the diapiric ascent of magmas or a combination of dyking and late ballooning (as exemplified by the recent articles in the Third Hutton Volume by Paterson et al., 1996; Petford, 1996; Weinberg, 1996). In the 1980's several papers appeared considering whether the softening of the wall rocks by heat released by the diapir would enhance the diapir's ability to penetrate the crust (the hot-Stokes models, e.g., Marsh, 1982; Morris, 1982; Emerman and Turcotte, 1984; Daly and Raefsky, 1985; Mahon et al., 1988; Miller et al., 1988). These authors found that the heat-content of single magma diapirs is insufficient to considerably enhance diapirism, because faster ascent rates are accompanied by faster cooling rates leading to early freezing of the diapir. More recently,

[1] Now at: Department of Earth Sciences, Oxford University, Parks Road, Oxford OX1 3PR, UK. Fax: +44.1865-272072.

PII S0040-1951(96)00269-7

diapirism has been shown to be more efficient than previously thought when the power-law rheology of the crust is taken into account (Weinberg and Podladchikov, 1994). Marsh (1982) suggested that if several diapirs followed the same path they could form a hot pathway allowing younger diapirs to rise increasingly higher before freezing. A related idea, derived mainly from field-based studies, is that of the nesting of diapirs into each other (e.g., Holder, 1979; Bouchez and Diot, 1990; Allen, 1992; Paterson and Vernon, 1995). Although these two ideas have been in the literature for some time, no previous work has explored in detail how and why several diapirs follow the same path, and how nested plutons could result from this process.

Tackley and Stevenson (1993) proposed a novel self-perpetuating mechanism of magma production by decompression melting in the asthenosphere. They noted that if an element of rock, partially molten or at the onset of melting, is given an infinitesimal velocity upwards, it will undergo decompression melting and density decrease, increasing the upward velocity. The system is thus unstable and upward movement will feed itself and lead to large-scale melting. In the present paper, this idea is applied to the crust, but rather than assuming zero heat flux to the base of the model as in Tackley and Stevenson (1993), constant temperature at the base of the model crust is assumed to explore the serial generation of diapirs, their rise and the decompression melting they may trigger.

Clemens and Vielzeuf (1987) argued that volatile phase-absent conditions predominate during high-grade metamorphism (upper amphibolite and granulite facies) of the lower and middle crust. Melting experiments have shown that the solidus temperatures of crustal and mantle rocks, at water undersaturated conditions, increase with depth (pressure) at a rate varying between 0 and 5°C/km depending on rock type and water content (Huang and Wyllie, 1973, 1975; Peterson and Newton, 1989; Parmentier and Morgan, 1990; Thompson, 1990; Johannes and Holtz, 1991). Thus, deep and hot rocks may melt if they are rapidly dragged upwards. Diapirs impose a convective movement in the crust by dragging surrounding rocks upwards and causing rocks further away to flow downwards to replace the ascending mass (Fig. 1). This convection has two important implications: (1) it may lead to decompression melting of the ascending rocks, and (2) it feeds the magma source with fresh, potentially fertile material that may remelt and originate a new diapir. This paper studies the consequences of decompression melting and renewal of the magma source caused by diapirism in the continental crust, by means of two-dimensional finite difference models. First decompression melting caused by the rise of a buoyant isolated diapir is studied; then the evolution of sequential diapirs originating at a partially molten layer at the base of a power-law crust is explored. The results may explain the origin of nested plutons or large upper crustal batholiths composed of several magmatic pulses, and the origin of gneiss domes with migmatite cores.

2. Computation and assumptions

The computer code used for the two-dimensional finite difference numerical simulations was developed by Harro Schmeling and was described in detail in Weinberg and Schmeling (1992) and Weinberg and Podladchikov (1995). The version of the code used here compares the temperature of every marker with that of a prescribed solidus curve, and determines whether the marker is molten. If a marker is warmer than the solidus temperature it becomes a new model phase (the partially molten rock) with new prescribed density (it is important to emphasize that, in contrast to Tackley and Stevenson (1993), the melting equations were not solved by the program so that the density of the partially molten rock could not be calculated, this limitation will be further discussed below). Similarly, if a marker was molten in the previous step but is now below the solidus temperature, it becomes a third model phase (the resolidified rock) with properties of its own. When the diapir surroundings undergo partial melting, they become part of the diapir and may have either similar or different properties to the initial diapir (here I will refer separately to the initial diapir and to the partially molten rock). In this paper only the densities of the three model phases were varied. Melting naturally decreases rock viscosity, but for simplicity and improved numerical results the viscosity of the partially molten rock was assumed equal to that of the solid, except in one case where the effect of viscosity decrease upon melting

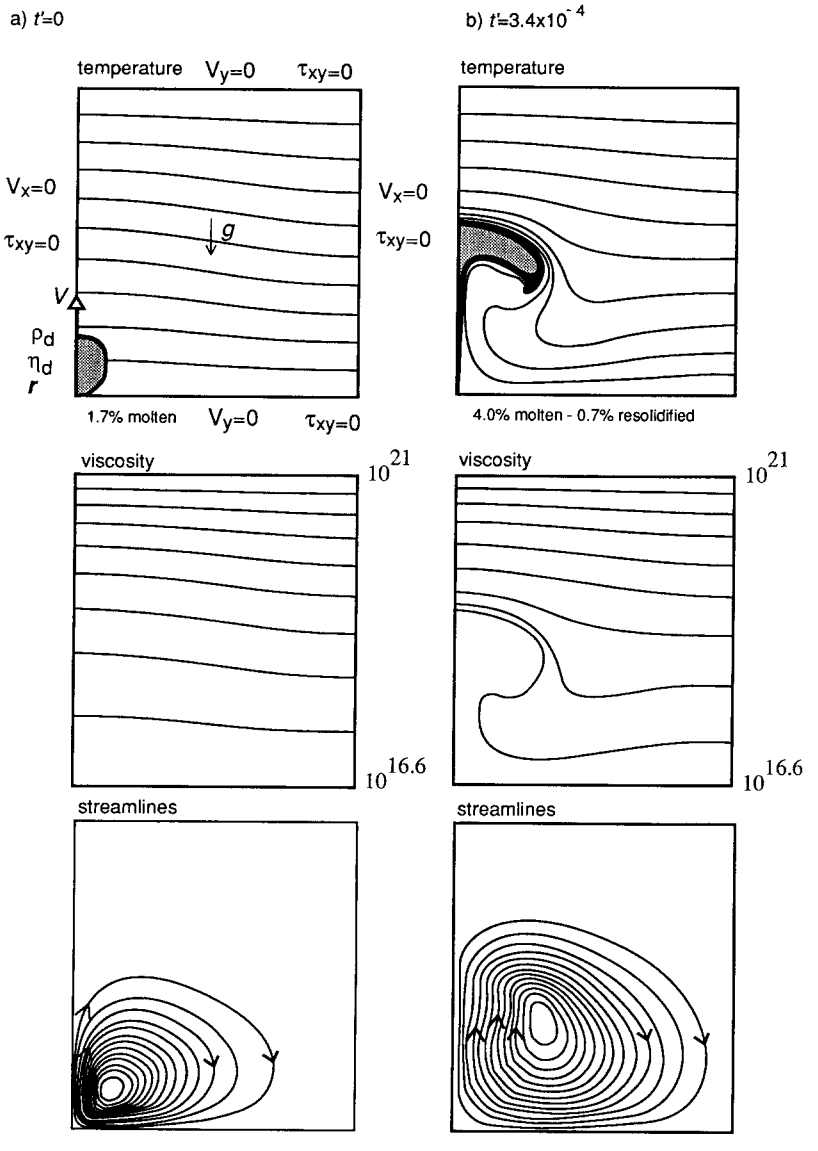

Fig. 1. (a) The initial set-up of the calculations; only half the box is shown because its sides are reflective. The initial temperature instability in the upper box had half a wavelength across the width of the box and an amplitude of 0.04 box heights. The initial diapir temperature, position and radius were constant: the temperature was equal to that of the base of the model, the radius was 1/10 of the total box height, and the initial position of the centre of the diapir was one radius above the bottom of the model, always on the side of the positive temperature instability. Each isotherm corresponds to 1/10 of the total temperature difference between top and bottom and each isoviscous line corresponds to half an order of magnitude change in viscosity. This calculation had viscosities varying from 4×10^{16} Pa s at the base to 10^{21} Pa s at the top (middle box), $\Delta\rho/\rho = 0.2$, and $R_c = 2000$ (see Table 1). The convective flow indicated by the streamlines in the bottom box is concentrated to the low-viscosity region of the model The aspect ratio of the box was 0.9, and corresponds to the characteristic aspect ratio for convection in systems with viscosity variation between top and bottom of the model of 2.5×10^4 Pa s (White, 1988). (b) The deflection of the isotherms and isoviscous lines by the rising diapir. The diapir grew in size due to the addition of partially molten surrounding rocks and is 2.7 times its initial volume including the resolidified material, and 2.3 times the volume considering only the partially molten rock (light grey, resolidified rocks in dark grey). Notice how the diapir tends to become a flat body as it rises through increasingly viscous crust. Dimensionless time $t' = t\kappa/h^2$.

was studied. It will be shown below that the low viscosity of the partially molten rocks has very little influence on the ascent of the diapir and on the system as a whole. This results from the relatively small influence of magma viscosity on the ascent velocity of diapirs (e.g., Weinberg and Podladchikov, 1994). However, melts of low viscosity (say $<10^5$ Pa s) may give rise to dykes totally changing the physical processes of transport and emplacement of the magmas generated (as explored in Weinberg, 1996). In this paper we disregard this possibility and concentrate on the evolution of diapirs. The two-dimensional geometry of the numerical models is likely to result in larger volumes of melt than would be expected for a three-dimensional calculation. This is because cylinders rise faster than spheres of similar radius, deflecting the isotherms more efficiently.

The initial diapir has a radius of 1/10 of the box height (Fig. 1) and may be viewed as composed by pure melt or by partially molten rock. Segregation of magma from the partially molten rock is not modelled here and the implications of this simplification will be discussed below. Furthermore, during melting and solidification no change in volume is computed. The temperatures at the top and bottom of the model crust were kept constant and the boundaries were free-slip and reflective (Table 1 and Fig. 1). The temperature at the top of the model was chosen arbitrarily to be 250°C. It is assumed here that this temperature corresponds to the brittle–ductile transition temperature so that the model only considers the viscous warm part of the crust (in nature the brittle–ductile transition is likely to cover a range of temperatures and depends on the flow-law parameters of the crust, and crustal stresses and strain rates). The constant temperature at the base of the models is the simplest boundary condition to study the serial generation of diapirs, and corresponds in nature to a crust repeatedly underplated by hot mantle basalts. For large viscosity variations across a convecting system ($>10^4$ Pa s; Stengel et al., 1982) convection is indifferent to whether the prescribed top boundary is free-slip or no-slip: in both cases the high-viscosity top part of the system behaves as an effective no-slip top boundary. Most calculations here involved Newtonian, temperature-dependent viscosity. The flow-law parameters were chosen to yield an upward viscosity increase across the model of 2.4×10^4 Pa s (a typical value for crustal rocks submitted to tectonic stresses). The dimensional values of top and bottom viscosities used in the models correspond to that of the power-law Westerly granite (Hansen and Carter, 1982) submitted to a tectonic strain rate of approximately 1.5×10^{-13} s^{-1}, for the prescribed temperatures (Table 1). (This is a fast regional tectonic strain rate but it simulates the effective viscosities of the Westerly granite around small diapirs; see discussion in Weinberg and Podladchikov, 1994.) The aspect ratio of the box was 0.9, equal to half the characteristic wavelength for convection in systems with such viscosity variation (from White, 1988). A few calculations using different aspect ratios con-

Table 1
Dimensional and dimensionless parameters for all models

Dimensional parameters			
$\alpha = 2 \times 10^{-7}$ K^{-1}	$r = 3$ km	$h = 30$ km	
$T_T = 250$°C	$T_{bottom} = 1000$°C	$\Delta T = 750$ K	
$\kappa = 10^{-6}$ m^2/s	$\rho = 2800$ kg/m^3	$\Delta\rho = 560$ kg/m^3	
Viscosities in Newtonian model (Figs. 1–3; in Pa s)			
$\eta_T = 1 \times 10^{21}$	$\eta_{bottom} = 4 \times 10^{16}$	$\Delta\eta = 2.50 \times 10^4$	$\bar{\eta} = 7.5 \times 10^{17}$
Viscosities in power-law model (Fig. 4; in Pa s)			
$\eta_{max} = 1 \times 10^{21}$	$\eta_{min} = 1.6 \times 10^{16}$	$\Delta\eta = 6.25 \times 10^4$	$\bar{\eta} = 4.4 \times 10^{17}$
Dimensionless parameters			
$\Delta\rho' = 0.2$	$\Delta T' = 0.2$	$T'_m = 1$ (Figs. 1–3)	
$T'_m = 0.96$ (Fig. 4)	$R_c = 2000$ (Figs. 1–3)	$R_c = 3400$ (Fig. 4)	

$\Delta\eta$ is the viscosity ratio between the top and bottom of the model. A low value was chosen for the thermal expansivity (α) of crustal rocks to minimise its influence (no thermal convection).

firmed that convection was fastest for this aspect ratio.

The number of markers in all calculations was 270 × 300, with a grid of 81 × 91 for the chemical field and 4 times greater resolution for the temperature field. The time step was kept smaller than the diffusion time across one temperature grid, or smaller than the time for marker displacement across one chemical grid. This resolution was found to be within the lower resolution limit for which diapir velocities converge, with an error of approximately ±2% (model diapir velocity is sensitive to both the chemical and the temperature fields, since the velocity of the top of the diapir is a combination of marker displacement and upward movement of the melting front due to decompression). With this resolution, the lower boundary layer during diapir ascent is approximately 5 chemical and 20 temperature grids thick.

3. Parameterization

One of the most important parameters controlling diapirism is the compositional Rayleigh number (R_c, defined by Schmeling, 1988 and modified here), which describes the ratio of the compositional buoyancy and dissipative effects of viscosity and heat conduction. R_c was found to be an important parameter determining the volume of decompression melting due to compositional convection (diapirism):

$$R_c = \frac{\Delta\rho g r^2 h}{\kappa \overline{\eta}}$$

where $\Delta\rho$ is the compositional density difference between diapir and wall rock (in kg/m^3), g the gravitational acceleration (in m/s^2), κ the thermal diffusivity (in m^2/s), and r is the diapir radius. Since this work does not consider the upper brittle layer of the crust, h is the height of the viscous part of the crust. $\overline{\eta}$ is the viscosity at the average temperature ($\overline{T}$) across the viscous crust (following Booker, 1976, who determined that when the viscosity for the mean temperature between top and bottom boundaries is used to calculate the Rayleigh number, the onset of convection and the measured heat-flux simulate convection with constant viscosity fluids). In the case of a power-law crust R_c may be estimated by finding the effective viscosity of the crust around the diapir at $\overline{T}$ (following Weinberg and Podladchikov, 1994):

$$\overline{\eta}_{\text{eff}} = \frac{6^{n-1}}{3^{(n+1)/2} A (\Delta\rho g r)^{n-1} e^{-E/R\overline{T}}}$$

where A is the pre-exponential parameter (in Pa^{-n} s^{-1}), E the activation energy (in kJ/mol), R the gas constant (in kJ/mol K), n the power-law exponent ($n = 1$ for Newtonian fluids) and $\overline{T}$ the average absolute temperature (in K).

Two other parameters are necessary to describe melting in the crust. One is the dimensionless solidus temperature gradient $\Delta T'$, defined as the ratio between the gradient of the solidus curve (dT_s/dz) and the geothermal gradient (dT_g/dz), both assumed to increase linearly with depth:

$$\Delta T' = \frac{dT_s/dz}{dT_g/dz}.$$

The range of values for $\Delta T'$ in the crust is likely to vary considerably due to wide variations in the two temperature gradients. Values between 0.1 and 0.3 seem the most reasonable for decompression models (e.g., negative values characteristic of water-saturated crust would not lead to decompression melting). The other parameter is the melting temperature at the base of the crust (T_m) nondimensionalized by the temperature at that depth (T_b): $T'_m = T_m/T_b$. (If $T'_m < 1$ the base of the model is partially molten, as in the model of Fig. 4, Table 1).

The initial temperature of the diapir (T_d), and its starting depth also affects decompression melting. Whereas T_d controls the warming up of the wall rocks, its initial depth controls the upward drag on the surrounding rocks. These two parameters were kept constant as indicated in Fig. 1. The dimensional values of all parameters used in the models are listed in Table 1.

4. Results

4.1. Decompression melting

Fig. 1 shows how a rising magma diapir can drive convection of the viscous crust and cause decompression melting of the wall rock which adds volume and buoyancy to the initial magma body. The upward movement and the deflection of the isotherms

(Fig. 1b) lead to strongest decompression melting directly beneath the diapir. Decompression melting during diapirism is studied here as a function of R_c. The density of the partially molten rock is assumed equal to that of the initial diapir. It is important to emphasise that it is not the degree of partial melt that is being calculated but simply the volume of rock that crosses the solidus curve. The degree of partial melting is implicitly assumed by the prescribed density.

When a diapir rises through a crust too cold to melt, the diapir cools and gradually loses its buoyancy and velocity. In a warm and dry crust, decompression melting of the surrounding rocks adds buoyancy to the diapir allowing faster and higher rise into the upper crust. Fig. 2 compares the development of three identical diapirs rising through crusts of the same rheology and temperature profiles. The difference between them is that decompression melting does not occur in one case, and the two other cases have different diapir viscosities. Whereas the two diapirs helped by melting rose approximately $5r$ before solidification, the diapir rising through solid crust travelled only $2.5r$. The small differences between the diapirs of high and low viscosities are surprising. Despite the fast initial velocity of the low-viscosity diapir, it froze before the more viscous diapir. This is because the low friction between the low-viscosity diapir and surroundings leads to a smaller flow cell on the surroundings and thus a smaller deflection of the isotherms. This in turn results in smaller volumes of decompressed rocks compared to the more viscous case (Fig. 2b). A conclusion from this model is that the viscosity decrease due to decompression melting of the surroundings is of little significance for diapiric ascent

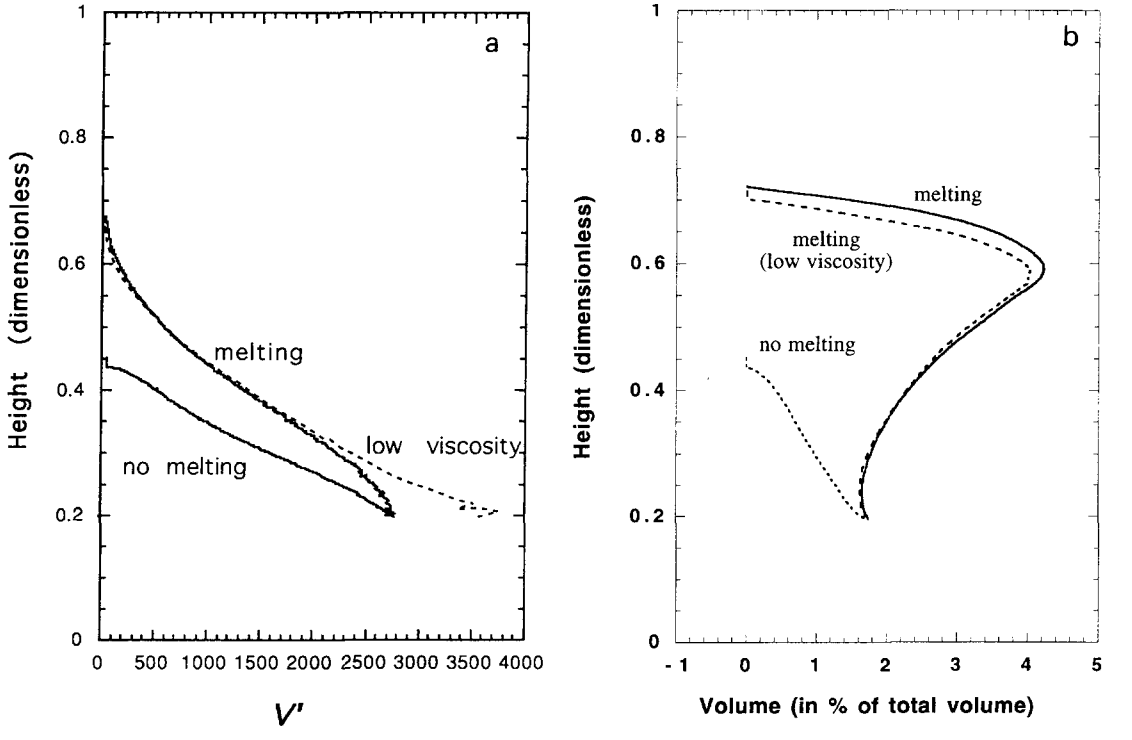

Fig. 2. (a) Dimensionless velocity ($V' = Vh/\kappa$), and (b) dimensionless volume of partially molten rock — a measure of buoyancy — as a function of height of the top of three diapirs of equal initial buoyancy rising through a crust of similar viscosity profile ($\Delta\rho/\rho = 0.2$, $R_c = 2000$). Decompression melting is prevented in one case (*no melting*), by increasing the solidus temperature of the model crust) and allowed in the two others. The difference between the two diapirs where decompression melting occurs is that in one the partially molten rock has a viscosity two orders of magnitude lower than the wall rock (at the same temperature), whereas in the other it has the same viscosity as the wall rock.

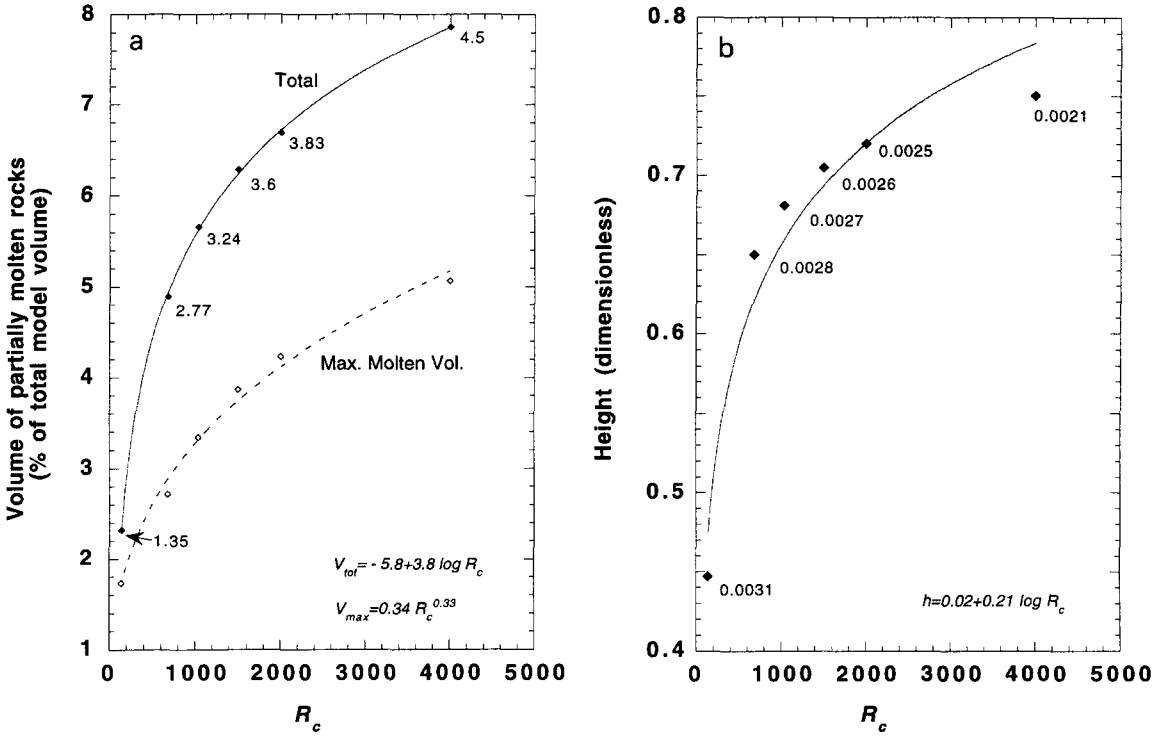

Fig. 3. (a) Total rock volume that went beyond the solidus during diapirism (measured after all melt is solidified, filled markers) and maximum volume of partially molten rock at any time during ascent (unfilled markers) as a function of R_c. Volumes are given as percent of total volume of the model crust. The numbers close to the filled markers correspond to the ratio between the initial and final diapir volume. (b) Height of the top of the diapir when solidification ends, at the dimensionless time ($t' = t\,\kappa/H^2$) given by the numbers in the plot, as a function of R_c. R_c was varied by shifting equally the viscosity at the top and bottom of the model (viscosity ratio between top and bottom, $\Delta\eta$, constant). In this model $\Delta\rho/\rho = 0.2$.

when compared to the more important increase in buoyancy.

Fig. 3 shows the results of a series of calculations aimed at determining the relation between R_c and the volume of partially molten rocks caused by diapirism, and the height reached by the diapir at the time of solidification. In these calculations resolidified rocks have the same density as the ambient rock and behave passively. Two volumes of partially molten rock are given for each calculation. One is the maximum volume of rock above the solidus at any time during ascent, a measure of the maximum buoyancy during ascent ('max. molten volume' in Fig. 3a). The other is the total volume of rock that underwent melting measured after all melt solidified ('Total' in Fig. 3a). The rate of increase in volume of partially molten rocks weakens as R_c increases. This is due to the upward exponential increase in viscosity of the crust, which causes a rapid deceleration of diapirs as they reach high model crustal levels (Fig. 3b). An immediate geological implication of the results is that decompression caused by the initial diapir may be able to trigger partial melting of wall-rock volumes several times its own volume. Heat provided to the surroundings (as in the hot-Stokes models) plays only a minor role.

4.2. Sequential diapirs from a molten layer at the base of a power-law crust

Another set of models explored the sequential diapirism originating from a partially molten layer at the base of a power-law crust. The power-law exponent $n = 2.9$ used in the model was that of the Westerly Granite determined by Carter et al. (1981). The values of E and A were changed to

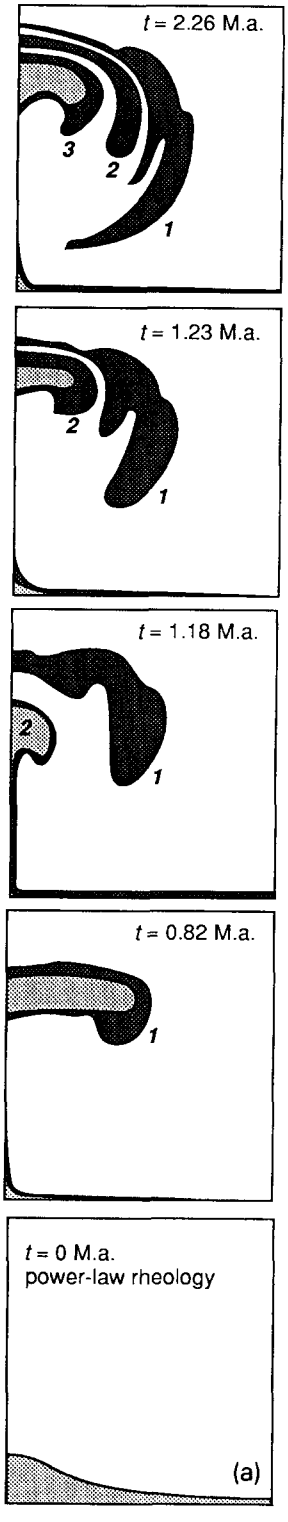

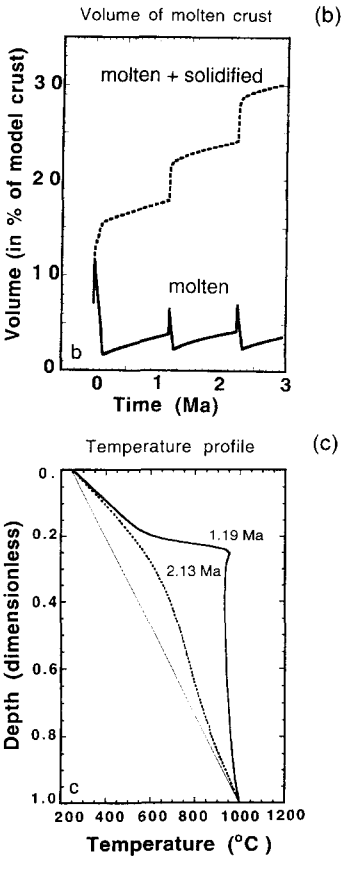

Fig. 4. (a) Five steps in a calculation in which three diapirs (numbered 1 to 3) leave a molten source at the base, and rise through power-law crust, melt some of the surroundings through decompression and spread close to the top of the model where the viscosity rapidly increases. The wall rock that undergoes melting has the same properties (and shading in the figure) as the initial diapir. The solidified parts of the diapir (in dark grey) has the same properties as the solid wall rocks and thus behave passively during further deformation imposed by the rise of younger diapirs. The initial amplitude of the partially molten layer in the lower box was prescribed. Viscosity in this model varies as a function of strain rate and temperature, from 10^{16} Pa s close to the hot diapir, to 10^{21} Pa s at the top of the model (Table 1, these values vary somewhat as the diapir rises). (b) Volume of partially molten crust in (a) as a function of time. The peaks of rapid melting correspond to the rise of diapirs and decompression melting of the wall-rock. The first diapir is more voluminous than the others as a result of the initial set-up of the model, whereas the second and third diapirs correspond to a more steady regime. (c) Two vertical temperature profiles across the centre of the second diapir on (a) compared to the undisturbed temperature profile (fine straight line). One profile shows the temperature at early emplacement stages of the diapir (1.19 Ma), and the other shows the remaining perturbation after 1 Ma, just before the third diapir starts to rise.

yield a viscosity range similar to that in Fig. 1 ($\log A = -8.8$ MPa^{-n} s^{-1}, $E = 79.5$ kJ/mol). In these models $T'_m = 0.96$ and $\Delta T' = 0.16$, so that the undisturbed partially molten layer is initially approximately 1.4 km thick. A thermal disturbance in the form of half a wavelength with an amplitude of 0.2 of the box height was introduced to trigger the first diapir (bottom box in Fig. 4a; the results of a calculation with an initial amplitude of 0.1 were identical, except for an incubation time of 0.1 Ma for the first diapir to start its ascent). The flow of the model crust associated with the rise of the first diapir causes decompression melting along the diapir's tail (increase in volume of partially molten rock shown by the first spike of Fig. 4b) and drives colder and fertile rocks downwards, to the base of the crust where they gradually warm up, melt and rise as a second diapir. This process results in a series of diapirs, each rising and melting the surroundings similarly to the isolated blobs studied above. The first diapir of the series is larger than the others due to the unstable initial set up of the models. Subsequent diapirs are smaller but increase in size with time as the crust becomes warmer due to heat advected by earlier diapirs. Fig. 4b shows the changes in the volume of partially molten model crust during diapir rise. First, there is a fast increase in volume (due to decompression melting) followed by a sharp decrease corresponding to the rapid freezing of the diapir at upper crustal levels. It follows a period of quiescence where the base of the crust slowly warms up and melts until the buoyancy becomes sufficiently high, decreasing the effective viscosity of the power-law crust and allowing another diapir to leave the source.

Fig. 4c shows the temperature profiles of the model crust just after the rise of the second diapir and just before the rise of the third diapir one million years later. The profiles show that the initial steady-state geothermal gradient of the model crust was strongly perturbed by the diapirs and that the perturbation lasted long enough to cause more voluminous melting under the path of previous diapirs and to control the site of renewed magma ascent. Similar qualitative results were found in a Newtonian model (not shown here).

The main result of this calculation is that, given a long-lasting heat supply to the base of the crust such as underplated basalts, the diapiric ascent of crustal magmas will cause renewal of the source, renewed melting and repetition of the process, resulting in a series of diapirs following the same path and nesting into each other in the upper crust.

5. Discussion

5.1. Model limitations

An important parameter controlling the results is the density of the partially molten crust. Since the computer code does not solve the melting equations this density had to be prescribed a priori. In nature, the melt fraction and the density of the partially molten rocks may change at different stages of the ascent of the diapir, adding a further variable to the problem. In the models the properties of the initial diapir and the partially molten wall rock were assumed equal; obviously this does not need to be the case in nature. The partially molten wall rock may either be lighter or denser than the initial diapir depending on composition and percentage of melt in each. If the partially molten rock, mainly at the diapir's tail, is lighter than the diapir, it will tend to rise into and across the diapir magma to occupy its top. Conversely if it is denser it will tend to occupy the bottom part and the core of the diapir during ascent (see Weinberg, 1992, for a detailed study of the distribution of magmas of different densities inside rising diapirs). In either case, the result is a zoned pluton.

Melt segregation from the partially molten wall rocks into the diapir was not modelled here. It is possible that once the melt in the partially molten rock becomes interconnected (melt fraction $>\sim 5\%$), it starts to segregate and migrate into the diapir. If the diapir rises rapidly as compared to typical segregation time scales, very little melt will be added to the diapir. However, as the diapir slows in colder crust, more melt may migrate into and inflate the diapir.

The next step in understanding the processes proposed here is to solve the melting equations and add melt segregation (as was done for the asthenosphere by Tackley and Stevenson, 1993). Despite the assumptions and simplifications the calculations capture the essence of a hitherto undescribed mechanism

for crustal melting that may enhance the penetration ability of diapirs, trigger melting and lead to sequential diapirism.

5.2. Decompression melting

The hot-Stokes diapir models established that although heat softening of the diapir's surroundings allows faster ascent rates, it also accelerates diapir cooling limiting the distance that magma diapirs rise before solidifying (e.g., Marsh, 1982; Mahon et al., 1988). Heat softening is effective when the velocity of the diapir is slow enough to produce a wide thermal boundary layer but fast enough to keep this boundary layer from becoming too wide. Ideal conditions for thermal softening were found to be between Peclet numbers ($Pe = Vr/\kappa$, where V is diapir velocity) of 1 and 100 (e.g., Daly and Raefsky, 1985). In contrast, decompression melting is favoured by, but not limited to, high Pe because this allows an effective upward bending of the isotherms without time for thermal reequilibration of the disturbance. Decompression melting can also occur for lower Pe since it depends also on other parameters such as the dimensionless solidus temperature gradient ($\Delta T'$) and dimensionless melting temperature at the base of the crust (T'_m). In most of the models above, the initial Pe of the diapirs was higher than 100, resulting in little heat loss and a narrow thermal aureole through most of the ascent. Melting was mostly due to decompression and restricted to the diapir's tail.

The results presented here suggest that given conditions where decompression melting may occur (hot crust, low solidus temperature, high diapir buoyancy), the initial diapir may cause the partial melting of wall rocks several times its own volume. In this way, the thermal and mechanical energy spent by the diapir during its ascent (by heating and dragging the wall rock) is partly recovered.

5.3. Sequential diapirism and nested plutons

Several zoned plutons, particularly those with sharp internal contacts, have been interpreted as resulting from the nesting of sequential diapirs (e.g., Holder, 1979; Tindle and Pearce, 1981; Ramsay, 1989; Bouchez and Diot, 1990; Allen, 1992). Particularly interesting is the case of the reversely zoned Turtle pluton in California where a schlieren zone several tens of metres wide and concentric with the outline of the pluton separates a core facies from a rim sequence (Allen, 1992). The schlieren zone is highly strained and composed of coarse-grained granodiorite, with a strong foliation and subvertical screens of wall-rock gneiss. The model proposed by her for the origin of the Turtle pluton is that it comprises two nested diapirs derived from a single magma chamber at depth, the first diapir (the rim sequence) being now separated from the second diapir (the core facies) by the highly deformed schlieren zone. Several zoned plutons show compositional pulses that are not related to a single parent magma but reflect different source materials or separately evolved magmas (e.g., Tindle and Pearce, 1981; Allen, 1992; Stephens, 1992), suggesting that they are not differentiated in situ but result from the emplacement of different magma pulses. Paterson and Vernon (1995) reviewed the data on several zoned plutons such as the Ardara, in Ireland, Cannibal Creek, in Australia and Pappoose Flat, in California, and argued based on the chemistry of the different magma pulses and on structural grounds that they resulted from the nesting of diapirs.

A direct consequence of sequential diapirism is the nesting of diapirs as they become trapped in the upper, stiffer upper crust (Fig. 4a). In the viscous models above, diapirs are unable to pierce through the surroundings. Therefore there is always a thin layer of wall rocks surrounding diapirs (Fig. 4) that separates the nested diapirs in a similar way to that observed in the Turtle pluton (Allen, 1992). For magma diapirs to pierce the crust and nest directly into each other, it is necessary to appeal to other mechanisms such as a combination of block stoping and assimilation.

The time gap between diapirs is a function of crustal viscosity, density decrease upon melting, heat flow into the base of the crust and heat diffusivity of crustal rocks, geothermal gradient and solidus temperature of crustal rocks. In Fig. 4, the temperature at the bottom of the model crust was kept constant. In nature, this needs not be the case. If the heat conducted to the base of the crust increases or decreases with time, each melting pulse becomes more or less voluminous and the time gap between pulses

might decrease or increase, respectively. Conditions in Fig. 4 were such that the time gap between diapirs was sufficiently large so that preceding diapirs are solid when younger ones leave the source, but sufficiently short so that the thermal disturbance had not totally vanished. The remaining disturbance allowed younger diapirs to rise faster through lower viscosity crust, and to solidify at slightly shallower levels than previous diapirs. Had the time gap been shorter, younger diapirs would have risen into a molten older diapir; had the time gap been longer, the lack of thermal disturbance caused by the first diapir would have allowed younger diapirs to initiate at a random position. The time gaps between the model diapirs are of the same order of magnitude as the 2 Ma time gaps between the three magma pulses in the Tuolomne pluton, California, revealed by detailed geochronological work (Kistler and Fleck, 1994). The sequential ascent of diapirs in the models might also explain the pulsating or even the periodic character of magmatic activity along volcanic arcs and large multipulse batholiths in the upper crust (Pitcher, 1993, p. 187).

Renewal of the source caused by the diapiric rise of magmas contrasts with the increasingly refractory nature of the source resulting from the removal of melt by an interconnected network of veins and dykes. Because dyking is unable to renew the source, melting will rapidly stop unless the source is renewed by other external processes (e.g., tectonic deformation), or by raising isotherms or water content. In nature, diapir-driven convection of the crust brings different rocks to the high-temperature magma source zone. Their melting gives rise to magmas of different geochemical signature compared to previous magma diapirs. The process modelled here suggests an origin to nested plutons which also explains the varied geochemical signature of each new pulse. In this model, the source point remains fixed, but rocks flow into it, melt and rise.

5.4. Gneiss domes

Although this paper has concentrated mainly on the rise of magmas, decompression melting may also result from the rise of light rocks such as gneisses (Weinberg and Podladchikov, 1995) and mantle plumes. The deeper parts of several gneiss domes

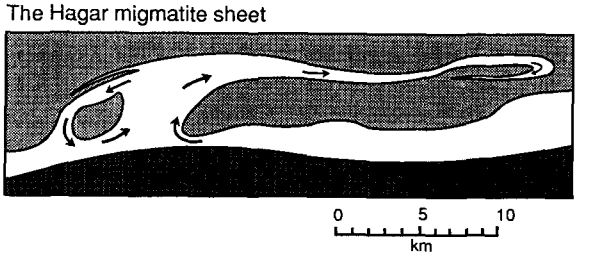

Fig. 5. Schematic convective movement of the Hagar migmatite sheet (in white) of east Greenland (as interpreted by Talbot, 1979). The basement is likely to be granulites (dark grey) and the rocks surrounding the migmatite sheet are metasediments (light grey).

are composed of migmatites (Talbot, 1979; Brun, 1983). The models here suggest that irrespective of which started first, doming or melting, the two processes reinforce each other. If the lower crust domes, its warmer parts may melt causing faster doming; conversely, if melting starts, buoyancy-driven doming may cause further melting. The gneisses and migmatites in Greenland form multiple sheets of migmatites, or recumbent folds which spread horizontally for tens of kilometres over metasedimentary rocks (Talbot, 1979 and references therein). Rather than being emplaced as the gneiss-cored nappes of the Swiss Alps from a single linear root zone, the gneiss sheets in Greenland seem to spread in a variety of directions, starting from the top of several linear centres in which nearly vertical movement occurred. The field descriptions and crustal sections presented by Talbot (Fig. 5) closely correspond to the two-dimensional models above, and were ascribed by him to some form of crustal convection. Detailed study of the area (structural mapping, determination of pressure–temperature–time paths) may provide comprehensive field support to the ideas put forward here.

In summary, the results above suggest that the combination of diapirism and decompression melting is an efficient way of melting large crustal volumes in a few million years. The result of this process may be nested plutons or flat mid- to upper-crustal multipulse batholiths, each pulse rising from the same point in the lower crust controlled by the thermal disturbance caused by the previous diapir. The batholith would typically be emplaced beneath extensional zones (caused by its own em-

placement) and would overlie a crust that has undergone some degree of convection. The batholith would be flanked by shortening zones in rocks of lower metamorphic grade (corresponding to the convection downwellings). Ideal crustal conditions for large melting events and diapirism are a warm and thick crust, with a steep geothermal gradient in the upper (brittle) crust, and high temperature but gentle geothermal gradient in the lower crust. These conditions may be found in Andean-type orogenic belts where the thermal profile is disturbed by intra- and under-plating of mantle-derived magmas. Although an external heat source may ultimately drive melting and diapirism, the volume of partially molten rock is not simply linked with the amount of heat flow into the crust. The amount of melt depends also on dynamical processes such as decompression melting of the wall rocks and on the renewal of the source by the crustal motion imposed by diapirs. Contrary to the perception expressed in Brown (1994), diapirism may be an efficient mechanism of magma transport through the viscous crust.

6. Conclusion

The idea of several diapirs following the same path and nesting into each other at emplacement level has been in the literature for nearly two decades. This paper studied this process. The models show that, given a long-lasting heat source at the base of the crust, the ability of one diapir to renew the magma source with fertile rocks to originate a new diapir leads to sequential diapirs that will nest into each other in the upper crust. The temperature disturbance caused by previous diapirs controls the position of ascent of new diapirs and may enhance their ability to penetrate the crust. Each magma pulse lasts 10^4–10^5 years, and the time in between pulses lasts 10^5–10^6 years. This process contrasts with magma ascent through dykes, where the source rapidly becomes refractory, and a new melt pulse requires either a renewal of the source through tectonic activity or an increase in temperature or water influx.

This paper studied also how decompression melting enhances diapirism and showed how the thermal and mechanical energy spent by the diapir may be partly regained in the form of increased buoyancy. This paper suggests that diapirism and decompression melting may interact to create favourable conditions for production, transport and emplacement in the upper crust of large volumes of felsic magmas. East Greenland with its domes and sheets of migmatites might provide a test area for the ideas above.

Acknowledgements

I would like to thank Prof. H. Schmeling for the discussions that led to some of the ideas put forward in this paper, as well as for developing the computer code used in the calculations. I would also like to thank Drs Mike Brown, Geoff Davies and Ross Griffiths for critical reading of an early version of the manuscript and Drs Rutter and van Keken for revising the manuscript.

References

Allen, C.M., 1992. A nested diapir model for the reversely zoned Turtle Pluton, southeastern California. Trans. R. Soc. Edinburgh, Earth Sci., 83: 179–190.

Booker, J.R., 1976. Thermal convection with strongly-dependent viscosity. J. Fluid Mech., 76: 741–754.

Bouchez, J.L. and Diot, H., 1990. Nested granites in question: contrasted emplacement kinematics of independent magmas in the Zaer pluton, Morocco. Geology, 18: 966–969.

Brown, M., 1994. The generation, segregation, ascent and emplacement of granite magma: the migmatite-to-crustally-derived granite connection in thickened orogens. Earth Sci. Rev., 36: 83–130.

Brun, J.-P., 1983. L'origine des domes gneissiques: modèles et tests. Bull. Soc. Geol. Fr., 25: 219–228.

Carter, N.L., Anderson, D.A., Hansen, F.D. and Kranz, R.L., 1981. Creep and creep rupture of granitic rocks. Am. Geophys. Union, Geophys. Monogr., 24: 61–82.

Clemens, J.D. and Vielzeuf, D., 1987. Constraints in melting and magma production in the crust. Earth Planet. Sci. Lett., 86: 287–306.

Clemens, J.D. and Mawer, C.K., 1992. Granitic magma transport by fracture propagation. Tectonophysics, 204: 339–360.

Daly, S.F. and Raefsky, A., 1985. On the penetration of a hot diapir through a strongly temperature-dependent viscosity medium. Geophys. J.R. Astron. Soc., 83: 657–681.

Emerman, S.H. and Turcotte, D.T., 1984. Diapiric penetration with melting. Phys. Earth Planet. Inter., 36: 276–284.

Hansen, F.D. and Carter, N.L., 1982. Creep of selected crustal rocks at a 1000 MPa. EOS, Trans. Am. Geophys. Union, 63: 437.

Holder, M.T., 1979. An emplacement mechanism for post-tectonic granites and its implications for their geochemical features. In: M.P. Atherton and J. Tarney (Editors), Origin of

Granite Batholiths, Geochemical Evidence. Shiva, Orpington, Kent, pp. 116–128.

Huang, W.L. and Wyllie, P.J., 1973. Melting relations of muscovite–granite to 35 kbar as a model for fusion of metamorphosed subducted oceanic sediments. Contrib. Mineral. Petrol., 42: 1–14.

Huang, W.L. and Wyllie, P.J., 1975. Melting reactions in the system $NaAlSi_3O_8$–$KAlSi_3O_8$–SiO_2 to 35 kilobars, dry and with excess water. J. Geol., 83: 737–748.

Johannes, W. and Holtz, F., 1991. Formation and ascent of granitic magmas. Geol. Rundsch., 80: 225–231.

Kistler, R.W. and Fleck, R.J., 1994. Field guide for a transect of the central Sierra Nevada, California: geochronology and isotope geology. U.S. Geol. Soc. Open-File Rep., 94-267, 50 pp.

Mahon, K.I., Harrison, T.M. and Drew, D.A., 1988. Ascent of a granitoid diapir in a temperature varying medium. J. Geophys. Res., 93: 1174–1188.

Marsh, B.D., 1982. On the mechanics of igneous diapirism, stoping, and zone melting. Am. J. Sci., 282: 808–855.

Miller, C.F., Watson, M.E. and Harrison, T.M., 1988. Perspectives on the source, segregation and transport of granitoid magmas. Trans. R. Soc. Edinburgh, Earth Sci., 79: 135–156.

Morris, S., 1982. The effects of a strongly temperature-dependent viscosity on slow flow past a hot sphere. J. Fluid Mech., 124: 1–26.

Parmentier, E.M. and Morgan, J.P., 1990. Spreading rate dependence of three-dimensional structure in oceanic spreading centres. Nature, 348: 325–328.

Paterson, S.R. and Fowler, Jr., T.K., 1993. Re-examining pluton emplacement processes. J. Struct. Geol., 15: 191–206.

Paterson, S.R. and Vernon, R.H., 1995. Bursting the bubble of ballooning plutons: a return to nested diapirs emplaced by multiple processes. Geol. Soc. Am. Bull., 107: 1356–1380.

Paterson, S.R., Fowler, Jr., T.K. and Miller, R.B., 1996. Pluton emplacement in arcs: a crustal-scale exchange process. Trans. R. Soc. Edinburgh, Earth Sci., 87: 115–125.

Peterson, J.W. and Newton, R.C., 1989. Reversed experiments on biotite–quartz–feldspar melting in the system KMASH: implications for crustal anatexis. J. Geol., 97: 465–485.

Petford, N., 1996. Dykes or diapirs? Trans. R. Soc. Edinburgh: Earth Sci., 87: 105–114.

Pitcher, W.S., 1993. The Nature and Origin of Granite. Chapman and Hall, London, 321 pp.

Ramsay, J.G., 1989. Emplacement kinematics of a granite diapir: the Chindamora batholith, Zimbabwe. J. Struct. Geol., 11: 191–209.

Schmeling, H., 1988. Numerical models of Rayleigh–Taylor instabilities superimposed upon convection. Bull. Geol. Inst. Univ. Uppsala, 14: 95–109.

Stengel, K.C., Oliver, D.S. and Booker, J.R., 1982. Onset of convection in a variable-viscosity fluid. J. Fluid Mech., 120: 411–431.

Stephens, W.E., 1992. Spatial, compositional, and rheological constraints on the origin of zoning in the Criffell pluton, Scotland. Trans. R. Soc. Edinburgh, Earth Sci., 83: 191–199.

Tackley, P.J. and Stevenson, D.J., 1993. A mechanism for spontaneous self-perpetuating volcanism on the terrestrial planets. In: D.B. Stone and S.K. Runcorn (Editors), Flow and Creep in the Solar System: Observations, Modeling and Theory. Kluwer, Dordrecht, pp. 307–321.

Talbot, C.J., 1979. Infrastructural migmatitic upwelling in east Greenland interpreted as thermal convective structures. Precambrian Res., 8: 77–93.

Thompson, A.B., 1990. Heat, fluids, and melting in the granulite facies. In: D. Vielzeuf and P. Vidal (Editors), Granulites and Crustal Evolution. Kluwer, Dordrecht, pp. 37–57.

Tindle, A.G. and Pearce, J.A., 1981. Petrogenetic modelling of in situ fractional crystallization in the zoned Loch Doon pluton, Scotland. Contrib. Mineral. Petrol., 78: 196–207.

Weinberg, R.F., 1992. Internal circulation in a buoyant two-fluid Newtonian sphere: implications for composed magmatic diapirs. Earth Planet. Sci. Lett., 110: 77–94.

Weinberg, R.F., 1994. Re-examining pluton emplacement processes: discussion. J. Struct. Geol., 16: 743–746.

Weinberg, R.F., 1996. The ascent mechanism of felsic magmas: news and views. Trans. R. Soc. Edinburgh, Earth Sci., 87: 95–103.

Weinberg, R.F. and Schmeling, H., 1992. Polydiapirs: multiwavelength gravity structures. J. Struct. Geol., 14: 425–436.

Weinberg, R.F. and Podladchikov, Y., 1994. Diapiric ascent of magmas through power-law crust and mantle. J. Geophys. Res., 99: 9543–9559.

Weinberg, R.F. and Podladchikov, Y.Y., 1995. The rise of solid-state diapirs. J. Struct. Geol., 17: 1183–1195.

White, D.B., 1988. The planforms and onset of convection with a temperature-dependent viscosity. J. Fluid Mech., 191: 247–286.